Available online at www.sciencedirect.com
SCIENCE DIRECT®
Tetrahedron: Asymmetry
Tetrahedron: *Asymmetry* 16 (2005) 2167–2171

Stereodifferentiation in the fluorescence of naproxen–arginine salts in the solid state

Ignacio Vayá, M. Consuelo Jiménez* and Miguel A. Miranda*

Departamento de Química, Instituto de Tecnología Química UPV-CSIC, Universidad Politécnica de Valencia, Camino de Vera s/n, 46071 Valencia, Spain

Received 21 April 2005; accepted 11 May 2005

Abstract—Three stereoisomeric salts of naproxen (NPX) with arginine (Arg), namely (*S*)-NPX/(*S*)-Arg, (*R*)-NPX/(*S*)-Arg and (*S*)-NPX/(*R*)-Arg, have been prepared, and their fluorescence spectra recorded in solution and in the solid state. While the emission properties in solution did not show significant differences with λ_{max} = 355 nm, τ_F (MeOH) ca. 11.5 ns and τ_F (H_2O) ca. 9 ns (as NPX/Na), the (*R*)-NPX/(*S*)-Arg and (*S*)-NPX/(*R*)-Arg solid salts displayed red-shifted fluorescence spectra with maxima at 375 nm and τ_F = 1.1 ns. By contrast, the behaviour of solid (*S*)-NPX/(*S*)-Arg was similar to that of NPX/Na with λ_{max} = 355 nm and τ_F ca. 5.5 ns. These results are explained based on the X-ray crystal structures and attributed to formation of NPX excimers emitting at longer wavelengths. Accordingly, such excimer emission was also observed in the fluorescence spectrum of a model NPX dyad in solution.

1. Introduction

Arylpropionic acids such as ibuprofen, naproxen, flurbiprofen and ketoprofen, belong to a family of non-steroidal anti-inflammatory drugs (NSAIDs), widely used as therapeutic agents for the treatment of a broad spectrum of pathophysiological conditions. These include very common processes such as fevers, headaches and pain caused by degenerative diseases, as well as osteo and rheumatoid arthritis.[1]

The activity of NSAIDs is associated with inhibition of the cyclooxygenase synthesis of the enzyme prostaglandin endoperoxide synthase (PGHS).[2,3] This enzyme, also known as cyclooxygenase or COX, is a membrane protein that catalyses in two steps the oxidation of arachidonic acid into hydroxy endoperoxide (PGH_2), which is the precursor of physiologically important agents such as thromboxanes, prostaglandins and prostacyclins. Two isoforms of COX are known, namely COX-1 and COX-2. The amino acid sequences of three COX-1 and four COX-2 enzymes obtained from different sources are known.[4] The residues at the cyclooxygenase binding site identified as being directly involved in the ligand–enzyme interaction include Arg (making a salt bridge) and Tyr (through hydrogen bonding).[5] This has been confirmed in the case of several COX-1 and COX-2 complexed with NSAIDs, whose structures have been resolved by X-ray crystallography.[4,6,7]

In order to gain further insight into the nature of drug–receptor interactions, the salts of an arylpropionic acid and arginine have been synthesised herein, to approach the situation in drug–COX complexes, and their behaviour studied by photophysical techniques. Among the NSAIDs, naproxen (NPX) was selected because its photophysical properties are well described. Thus, the possibilities of the first NPX singlet excited state to be used as reporter for the interaction of the drug with Arg have been explored. At this point it is worth mentioning that the anti-inflammatory activity of NPX is mainly associated with the (*S*)-isomer.[8] For this reason, it seemed worthwhile comparing the photophysical behaviour of the known (*S*)-NPX/(*S*)-Arg salt[9] with that of its (*R*,*S*)-isomer, that has not been previously described. To enhance the drug–amino acid interaction, the measurements have been performed on solid samples; the results have been discussed in connection with the X-ray structures, which are reported here for the first time.

* Corresponding authors. Tel.: +34 96 387 7340; fax: +34 96 387 7349; e-mail addresses: mcjimene@qim.upv.es; mmiranda@qim.upv.es

0957-4166/$ - see front matter © 2005 Published by Elsevier Ltd.
doi:10.1016/j.tetasy.2005.05.018

2. Results and discussion

The preparation of (*S*)-NPX/(*S*)-Arg and (*R*)-NPX/(*S*)-Arg (Scheme 1) was achieved by mixing equimolar amounts of (*S*)- or (*R*)-naproxen with (*S*)-arginine in deionised water. After removal of the solvent, the residue was recrystallised from methanol/acetonitrile.

The structural assignment was based on ^{1}H NMR, ^{13}C NMR, IR and X-ray crystallography.

2.1. Fluorescence studies

Fluorescence spectra of (*S*)-NPX/(*S*)-Arg and (*R*)-NPX/(*S*)-Arg were first performed in solution (water and methanol), under nitrogen. For comparison, parallel experiments were carried out for the sodium salt of (*S*)-naproxen, (*S*)-NPX/Na, under the same conditions. In all cases, the absorbance was 0.2 at the excitation wavelength (265 nm). The shape and position of the emission bands (centred at 350 nm), together with the fluorescence lifetimes of the two NPX–Arg salts (Table 1, entries 1, 2, 4 and 5) matched with those of the NPX sodium salt (Table 1, entries 3 and 6). These results can be attributed to the fact that the interaction occurring between the two counterions of the salt in solution is relatively weak due to solvation.

In order to enhance the drug–amino acid interaction, the fluorescence spectra of (*S*)-NPX/(*S*)-Arg and (*R*)-NPX/(*S*)-Arg were recorded in the solid state. In the former, the emission band displayed a maximum at 355 nm, very similar to the value obtained for solid (*S*)-NPX/Na; by contrast, (*R*)-NPX/(*S*)-Arg emitted at markedly longer wavelength (375 nm). The spectra of both salts are shown in Figure 1. Concerning the fluorescence lifetimes (measured at the emission maxima), a significant difference was found in the behaviour of the two diastereomers: while the (*S*,*S*)-salt had a τ_F value of 5.4 ns (Table 1, entry 7) very close to that of (*S*)-NPX/Na (5.8 ns, Table 1, entry 10) the (*R*,*S*)-isomer exhibited a much shorter τ_F (1.1 ns, Table 1, entry 8). Thus, a significant stereodifferentiation was observed for the decay process, indicating a much more efficient deactivation of the NPX singlet in (*R*)-NPX/(*S*)-Arg than in (*S*)-NPX/(*S*)-Arg. To rule out the possibility that this observation could be attributable to the presence of impurities in (*R*)-NPX/(*S*)-Arg, the salt (*S*)-NPX/(*R*)-Arg (with inverted configuration in both stereocentres) was prepared, and its emission spectra were measured in the solid state (see Table 1, entry 9 and Fig. 1). As expected for the two enantiomers, their photophysical properties were identical, confirming that their anomalous behaviour was not an artefact. Moreover, the fluorescence spectra measured for equimolar mixtures of (*R*)-NPX and (*S*)-Arg or (*S*)-NPX and (*S*)-Arg were identical to each other (in position and lifetime); they closely matched the spectrum of (*S*)-NPX/Na. Thus, the observed differences between the photophysical behaviour of the diastereomeric Arg salts in the solid state must be attributed to specific interactions experienced by the NPX chromophore in the crystalline microenvironment.

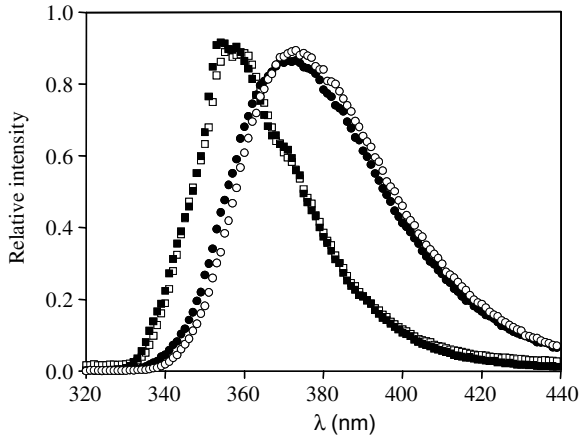

Figure 1. Fluorescence spectra of (*S*)-NPX/Na (□), (*S*)-NPX/(*S*)-Arg (■), (*R*)-NPX/(*S*)-Arg, (●) and (*S*)-NPX/(*R*)-Arg (○) in the solid state.

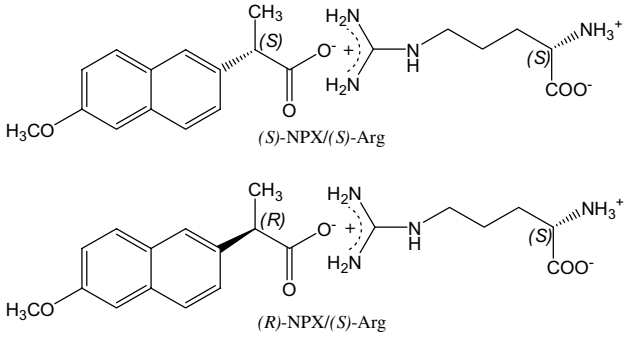

Scheme 1. Structural formulae of (*S*)-NPX/(*S*)-Arg and (*R*)-NPX/(*S*)-Arg.

Table 1. Fluorescence lifetimes of (*S*)-NPX/(*S*)-Arg, (*R*)-NPX/(*S*)-Arg, (*S*)-NPX/(*R*)-Arg and (*S*)-NPX/Na salts under different conditions

Entry	Compound	Conditions	τ_F (ns)
1	(*S*)-NPX/(*S*)-Arg	H_2O	9.2
2	(*R*)-NPX/(*S*)-Arg	H_2O	9.1
3	(*S*)-NPX/Na	H_2O	9.0
4	(*S*)-NPX/(*S*)-Arg	CH_3OH	11.5
5	(*R*)-NPX/(*S*)-Arg	CH_3OH	11.4
6	(*S*)-NPX/Na	CH_3OH	11.4
7	(*S*)-NPX/(*S*)-Arg	Solid	5.4
8	(*R*)-NPX/(*S*)-Arg	Solid	1.1
9	(*S*)-NPX/(*R*)-Arg	Solid	1.1
10	(*S*)-NPX/Na	Solid	5.8

2.2. X-ray structures

In order to ascertain whether the differences found in the fluorescence spectra in the solid state can be attributed to a different spatial arrangement of the counterpartners in the ionic network, single crystals of (*S*)-NPX/(*S*)-Arg and (*R*)-NPX/(*S*)-Arg were obtained, and their structures resolved by X-ray crystallography (see unit cells in Figs. 2 and 3).

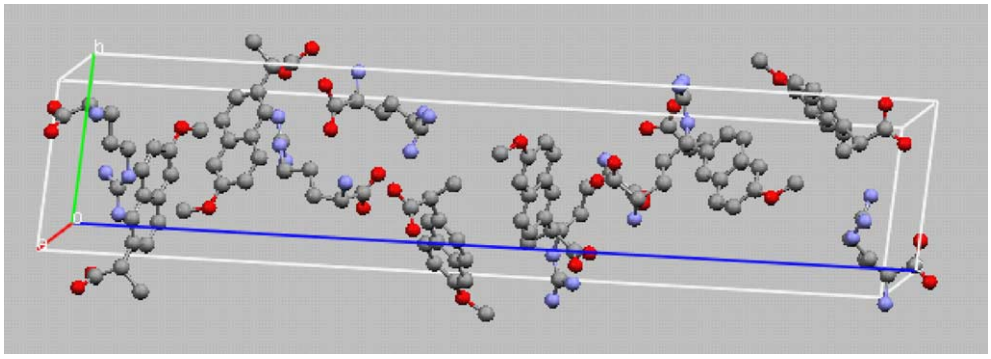

Figure 2. Unit cell for (*S*)-NPX/(*S*)-Arg.

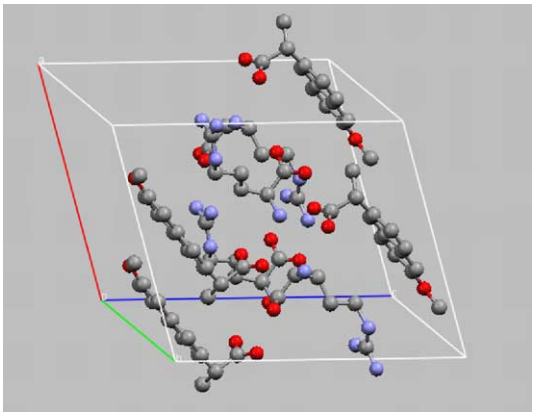

Figure 3. Unit cell for (*R*)-NPX/(*S*)-Arg.

The results showed that both salts crystallise in different spatial groups (trigonal and monoclinic, see Table 2).

A closer look at the crystal structures revealed that the main feature with potential photophysical implications was the NPX to NPX interaction, due to the relative spatial arrangement of different units of this chromophore in the network. Thus, in the case of (*R*)-NPX/(*S*)-Arg (Fig. 3) all the NPX moieties are parallel to each other and close enough as to produce excimer emission, while in the case of (*S*)-NPX/(*S*)-Arg (Fig. 2) the observed non-parallel arrangement prevents an efficient interaction between different naphthalene rings. In principle, an exciplex formation between NPX and Arg was unexpected, as this type of interaction is associated with a certain degree of charge transfer that requires the presence of free amino groups as donors. Obviously, this is not possible in the NPX/Arg salts, where only ammonium ions are present.

Table 2. Crystallographic data for (*S*)-NPX/(*S*)-Arg and (*R*)-NPX/(*S*)-Arg

	(*S*)-NPX/(*S*)-Arg	(*R*)-NPX/(*S*)-Arg
Empirical formula	$C_{40}H_{56}N_8O_{10}$	$C_{20}H_{28}N_4O_5$
Crystal system	Monoclinic	Trigonal
Space group	*C* 2	*P* 32 2 1
Unit cell dimensions	*a* = 14.662(5) Å	*a* = 9.145(5) Å
	b = 9.225(5) Å	*b* = 9.145(5) Å
	c = 17.129(5) Å	*c* = 43.307(5) Å
	α = 90.000(5)°	α = 90.000(5)°
	β = 113.865(5)°	β = 90.000(5)°
	γ = 90.000(5)°	γ = 120.000(5)°

2.3. Excimer emission in a model dyad

As stated above, the new emission of (*R*)-NPX/(*S*)-Arg and (*S*)-NPX/(*R*)-Arg at longer wavelength can be assigned to a NPX excimer. In order to check this hypothesis, the fluorescence of solutions containing increasing amounts of NPX (from 4×10^{-5} M to 0.1 M) were measured. However, this was not enough to generate the excimer, and the shape and the position of the spectral band (λ_{max} = 355 nm) indicated that only the monomer was emitting. To force a stronger interaction, a bichromophoric dyad containing two covalently bound NPX-related subunits[10] (Scheme 2) was prepared and spectroscopically characterised with its fluorescence properties studied.

The fluorescence behaviour of the dyad in acetonitrile was compared with that of NPX in the same solvent; the normalised spectra are shown in Figure 4. In both cases, the emission maxima appear at λ = 355 nm; however, the shape of the bands is different at longer wavelengths, indicating that a new species is also emitting in the dyad. The difference between the above normalised spectra allowed us to obtain the fluorescence spectrum of the new species (Fig. 4 inset), which can be attributed to the NPX-like excimer. Taking into account the different nature of the medium (solution vs crystalline state) it is reasonably similar to the traces shown in Figure 1 for (*R*)-NPX/(*S*)-Arg and (*S*)-NPX/(*R*)-Arg in the solid state.

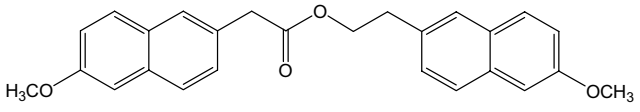

Scheme 2. Structural formula of the model dyad.

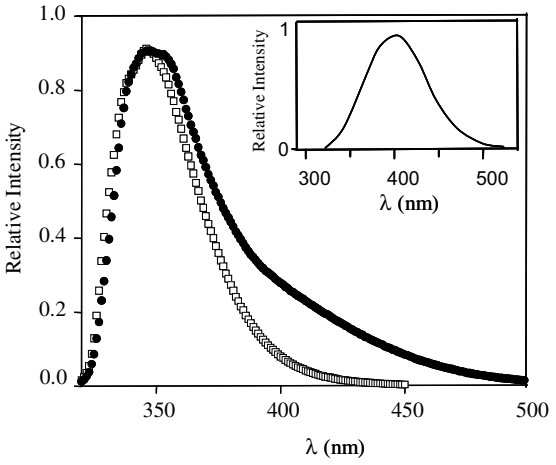

Figure 4. Normalised fluorescence spectra of (*S*)-NPX (□), and the model dyad (●) in acetonitrile (λ_{exc} = 266 nm). Inset: fluorescence spectrum of the excimer obtained by difference between the normalised spectra of (*S*)-NPX and that of the model dyad.

3. Conclusions

Three diastereomeric salts of naproxen with arginine have been prepared, and their fluorescence spectra recorded in solution and in the solid state. Their emission properties in solution did not show significant differences, however the (*R*)-NPX/(*S*)-Arg and (*S*)-NPX/(*R*)-Arg solid salts displayed red-shifted fluorescence and a τ_F value shorter than those of (*S*)-NPX/(*S*)-Arg and (*R*)-NPX/Na. This stereodifferentiation is explained based on the X-ray crystal structures and attributed to formation of NPX excimers emitting at longer wavelengths. Such excimer emission has also been observed in the fluorescence spectrum of a model NPX dyad in solution.

4. Experimental section

4.1. General

Isolation and purification were done by recrystallisation. UV spectra were recorded in water or acetonitrile; λ_{max} (nm) and log ε values (in parentheses) are given for each absorption band. IR spectra were obtained with a FTIR instrument; ν_{max} (cm^{-1}) is given for all the absorption bands. ^1H NMR and ^{13}C NMR spectra were measured in D_2O or $CDCl_3$ with a 300 MHz instrument; chemical shifts are reported in δ (ppm) values. Mass spectra were determined under electron impact; the ratios *m*/*z* and the relative intensities (%) are indicated for the significant peaks.

4.2. Synthesis of the substrates

To a solution of 173 mg (1 mmol) of (*S*)-arginine in deionised water (10 mL), 230 mg (1 mol) of (*S*)- or (*R*)-naproxen were added as a solid. The mixture was maintained under stirring for 30 min, the solvent removed under vacuum and the crude solid recrystallised from a 1:1 mixture of methanol and acetonitrile. The reaction was nearly quantitative. The crystals obtained following this procedure were suitable for X-ray characterisation. Crystallographic data (excluding structure factors) for the structures of (*S*)-NPX/(*S*)-Arg and (*R*)-NPX/(*S*)-Arg have been deposited with the Cambridge Crystallographic Data Centre as supplementary publication numbers CCDC 269482 and CCDC 269481, respectively.

4.3. Fluorescence measurements

Emission spectra were recorded on a spectrofluorimeter system, provided with a monochromator in the wavelength range 200–900 nm. For the experiments in solution, the samples were placed into $10 \times 10\ mm^2$ Suprasil quartz cells with a septum cap. The samples were purged with nitrogen for at least 15 min before the measurements. The absorbance of the samples at the excitation wavelength was kept at 0.2. In the solid state, $2 \times 10\ mm^2$ Suprasil quartz cells were used. Excitation and emission slits were maintained unchanged during the emission experiments. For time resolved fluorescence decay measurements, the conventional single photon counting technique was used.

4.4. Spectral data of the compounds

4.4.1. (*S*)-Arginine, mono[(*S*)-6-methoxy-α-methyl-2-naphthalene acetate] (*S*)-NPX/(*S*)-Arg. White crystals, mp 189–202 °C with decomposition. UV 230 (4.83), 262 (3.72), 272 (3.71), 318 (3.14), 330 (3.22); FTIR 3552, 3481, 3413, 3236, 1637, 1618, 1387, 1122, 621, 476; ^1H NMR 7.73–7.67 (d + d, J = 8.4 Hz, 2H, 4,8-ArH), 7.62 (br s, 1H, 1-ArH), 7.35 (dd, J_1 = 8.4 Hz, J_2 = 1.8 Hz, 1H, 3-ArH), 7.22 (br s, 1H, 5-ArH), 7.08 (dd, 1H, J_1 = 9.6 Hz, J_1 = 2.7 Hz, 7-ArH), 3.81 (s, 3H, OCH_3), 3.68–3.59 (q + t, 2H, C*H*CH_3, C*H*NH_3), 3.06 (t, J = 6.2 Hz, 2H, CH_2NH), 1.75 (m, 2H, CH_2CHNH_3), 1.53 (m, 2H, NHCH_2CH_2), 1.35 (d, J = 7.2 Hz, 3H, CHCH_3); ^{13}C NMR 183.7 (CH_3CH*C*OO^-), 174.1 (NH_2CH*C*OO^-), 156.3 (6-C), 138.6 (2-C), 132.7 (4a-C), 129.1–126.6 (8-CH, 8a-C, 4-CH, 9-CH), 125.0 (2-C), 118.0 (7-CH), 105.9 (5-CH), 55.0 (OCH_3), 54.0 ($CHNH_2$), 48.2 ($CHCH_3$), 40.1 (CH_2NH), 27.2 (CH_2CH_2CH), 23.5 (CH_2CH_2CH), 18.0 ($CHCH_3$).

4.4.2. (*S*)-Arginine, mono[(*R*)-6-methoxy-α-methyl-2-naphthalene acetate] (*R*)-NPX/(*S*)-Arg. White crystals, mp 188–201 °C with decomposition. UV 230 (4.83), 262 (3.71), 272 (3.71), 318 (3.14), 330 (3.22); FTIR 3552, 3481, 3413, 3236, 1637, 1618, 1387, 1118, 619, 471; ^1H NMR 7.70–7.65 (d + d, J = 9 Hz, 2H, 4,8-ArH), 7.59 (br s, 1H, 1-ArH), 7.31 (dd, J_1 = 8.7 Hz, J_2 = 1.8 Hz, 1H, 3-ArH), 7.20 (br s, 1H, 5-ArH), 7.05 (d, 1H, J_1 = 9.0, J_2 = 2.4 Hz, 7-ArH), 3.78 (s, 3H, OCH_3), 3.65–3.57 (q + t, 2H, C*H*CH_3, C*H*NH_2), 3.06 (t, J = 6.9, 2H, CH_2NH), 1.73 (m, 2H, CH_2CHNH_2), 1.50 (m, 2H, NHCH_2CH_2), 1.31 (d, 3H, J = 7.2 Hz, CHCH_3); ^{13}C NMR 183.7 (CH_3CH*C*OO^-), 174.1 (NH_2CH*C*OO^-), 156.3 (6-C), 138.6 (2-C), 132.7 (4a-C), 129.1–126.6 (8-CH, 8a-C, 4-CH, 9-CH), 125.0 (2-CH), 118.0 (7-CH), 105.9 (5-CH), 55.0 (–OCH_3), 54.0

(–$CHNH_2$), 48.2 (–$CHCH_3$), 40.1 (CH_2NH), 27.2 (CH_2CH_2CH), 23.5 (CH_2CH_2CH), 18.0 ($CHCH_3$).

4.4.3. (*R*)-Arginine, mono[(*S*)-6-methoxy-α-methyl-2-naphthalene acetate] (*S*)-NPX/(*R*)-Arg. White crystals, mp 188–202 °C with decomposition. UV 230 (4.83), 262 (3.71), 272 (3.71), 318 (3.14), 330 (3.22); FTIR 3552, 3481, 3413, 3236, 1637, 1618, 1387, 1122, 621, 476; ^{1}H NMR 7.76–7.71 (d + d, $J = 8.4$, 2H, 4,8-ArH), 7.66 (br s, 1H, 1-ArH), 7.40 (dd, $J_1 = 8.4$ Hz, $J_2 = 1.8$ Hz, 1H, 3-ArH), 7.26 (br s, 1H, 5-ArH), 7.11 (dd, 1H, $J_1 = 9$ Hz, $J_2 = 2.3$ Hz, 7-ArH), 3.84 (s, 3H, OCH_3), 3.72–3.63 (q + t, 2H, $CHCH_3$, $CHNH_2$), 3.14 (t, 2H, $J = 6.9$, CH_2NH), 1.80 (m, 2H, CH_2CHNH_2), 1.55 (m, 2H, $NHCH_2CH_2$), 1.38 (d, 3H, $J = 6.9$ Hz, $CHCH_3$); ^{13}C NMR 183.6 (CH_3CHCOO^-), 174.1 (NH_2CHCOO^-), 156.3 (6-CO), 138.6 (2-C), 132.7 (4a-C), 129.1–126.5 (8-CH, 8a-C, 4-CH, 9-CH), 125.0 (2-CH), 118.0 (7-CH), 105.9 (5-CH), 55.0 (–OCH_3), 54.0 (–$CHNH_2$), 48.2 (–$CHCH_3$), 40.1 (CH_2NH), 27.2 (CH_2CH_2CH), 23.5 (CH_2CH_2CH), 18.0 ($CHCH_3$).

4.4.4. 2-(2-Methoxynaphthalen-6-yl)ethyl-2-(2-methoxynaphthalen-6-yl) acetate. White crystals; UV 230 (4.92), 262 (4.10), 272 (4.12), 318 (3.60), 330 (3.70); FTIR 3551, 3478, 3412, 3236, 1637, 1617, 1265, 1133, 619, 481; ^{1}H NMR 7.64–7.48 (m, 6H, 1,4,8-ArH and 1′,4′,8′-ArH), 7.32–7.20 (dd + dd, $J_1 = 8.7$ Hz, $J_2 = 2.1$ Hz and $J_1 = 8.4$ Hz, $J_2 = 1.8$, 1H, 3-ArH and 3′-ArH), 7.14–7.08 (m, 4H, 5,7-ArH and 5′,7′-ArH), 4.39 (t, 2H, $J = 6.9$, CH_2O), 3.93 and 3.92 (s + s, 6H, OCH_3), 3.72 (s, 2H, CH_2CO), 3.04 (t, $J = 6.9$ Hz, 2H, CH_2CH_2O); ^{13}C NMR 172.0 (CH_2COO), 157.9, 158.0 (6-C and 6′-C), 133.1–105.9 (aromatic C and CH), 65.6 (CH_2COO), 55.6 (OCH_3), 41.8 (CH_2CO), 35.3 (CH_2CH_2O); MS 400.30 (M^+, 4%), 216.30 (9%), 185.3 (16%), 184.29 (100%), 172.2 (10%), 171.20 (41%), 141.20 (10%), 128.00 (23%), 115.20 (7%), 79.20 (60%).

Acknowledgements

The UPV (PI 2003-0522 and predoctoral fellowship to I.V.), the MYCT (Grant CTQ2004-03811) the Generalitat Valenciana (Grupos03/082 and GV04B-468) are gratefully acknowledged for financial support. We also thank our colleague Dr. M. L. Marin for providing a gift of (2-methoxynaphthalen-6-yl)acetic acid and Dr. A. Llamas (Unidade de Raios X de la Universidade de Santiago de Compostela) for the X-ray measurements.

References

1. Sondhi, S. M.; Rajvanshi, S.; Singh, N.; Jain, S.; Lahoti, A. M. *Centr. Eur. J. Chem.* **2004**, *2*, 141–187.
2. Dannhardt, G.; Kiefer, W. *Eur. J. Med. Chem.* **2001**, *36*, 109.
3. Bhattacharyya, D. K.; Lecomte, M.; Rieke, C. J.; Garavito, C. J.; Smith, W. L. *J. Biol. Chem.* **1996**, *271*, 2179.
4. Kiefer, J. R.; Pawlitz, J. L.; Moreland, K. T.; Stegeman, R. A.; Hood, W. F.; Gierse, J. K.; Stevens, A. M.; Goodwin, D. C.; Rowlinson, S. W.; Marnett, L. J.; Stallings, W. C.; Kurumbail, R. G. *Nature* **2000**, *405*, 97.
5. Kurumbail, R. G.; Stevens, A. M.; Gierse, J. K.; McDonald, J. J.; Stegeman, R. A.; Pak, J. Y.; Gildehaus, D.; Miyashiro, J. M.; Penning, T. D.; Seibert, K.; Isakson, P. C.; Stallings, W. C. *Nature* **1996**, *384*, 644.
6. Di Marco, S.; Priestle, J. P.; Grüter, M. G.; Wennogle, L. P.; Boyar, W. *Acta Crystallogr. D* **1997**, *53*, 224.
7. Picot, D.; Loll, P. J.; Garavito, R. M. *Nature* **1994**, *367*, 243.
8. Evans, A. M. *J. Clin. Pharmacol.* **1996**, *36*, 7S.
9. Fried, John H.; Harrison, Ian T US 73-372028 19730621.
10. Ekuribe, N. N.; Dyanov, T. A. U. S. Patent 99-161864 19991027.